Brazilian Journal
of Chemical
Engineering

ISSN 0104-6632
Printed in Brazil

Vol. 21, No. 04, pp. 531 - 544, October - December 2004

TWO-PHASE AQUEOUS MICELLAR SYSTEMS - AN ALTERNATIVE METHOD FOR PROTEIN PURIFICATION

C. O. Rangel-Yagui[1,*], A. Pessoa-Jr[1], and D. Blankschtein[2]

[1]Department of Biochemical and Pharmaceutical Technology /FCF, University of São Paulo,
Av. Prof. Lineu Prestes, 580 - Bloco 16, CEP 05508-950, Phone (11) 3091-3710,
Fax: (11) 3094-3694, São Paulo - Brazil.
E-mail: corangel@usp.br
[2]Department of Chemical Engineering, Massachusetts Institute
of Technology, Cambridge, MA, USA.

(Received: November 10, 2003 ; Accepted: July 7, 2004)

Abstract - Two-phase aqueous micellar systems can be exploited in separation science for the extraction/purification of desired biomolecules. This article reviews recent experimental and theoretical work by Blankschtein and co-workers on the use of two-phase aqueous micellar systems for the separation of hydrophilic proteins. The experimental partitioning behavior of the enzyme glucose-6-phosphate dehydrogenase (G6PD) in two-phase aqueous micellar systems is also reviewed and new results are presented. Specifically, we discuss very recent work on the purification of G6PD using: i) a two-phase aqueous micellar system composed of the nonionic surfactant *n*-decyl tetra(ethylene oxide) ($C_{10}E_4$), and (ii) a two-phase aqueous mixed micellar system composed of $C_{10}E_4$ and the cationic surfactant decyltrimethylammonium bromide (C_{10}TAB). Our results indicate that the two-phase aqueous mixed ($C_{10}E_4$/C_{10}TAB) micellar system can improve significantly the partitioning behavior of G6PD relative to that observed in the two-phase aqueous $C_{10}E_4$ micellar system.
Keywords: two-phase aqueous micellar systems, protein purification, excluded-volume interactions, electrostatic interactions.

INTRODUCTION

Surfactants are amphiphlilic molecules composed of a hydrophilic or polar moiety known as head and a hydrophobic or nonpolar moiety known as tail. The surfactant head can be charged (anionic or cationic), dipolar (zwitterionic), or noncharged (nonionic), and the surfactant tail is a linear hydrocarbon chain in the surfactants considered in this paper (Tanford, 1980). When surfactant molecules are dissolved in water at concentrations above the critical micelle concentration (CMC), they form aggregates known as micelles. In a micelle, the hydrophobic tails flock to the interior in order to minimize their contact with water, and the hydrophilic heads remain on the outer surface in order to maximize their contact with water (see Figure 1) (Chevalier and Zemb, 1990; Tanford, 1980). The micellization process in water results from a delicate balance of intermolecular forces, including hydrophobic, steric, electrostatic, hydrogen bonding, and van der Waals interactions. The main attractive force results from the hydrophobic effect associated with the nonpolar surfactant tails, and the main opposing repulsive force results from steric interactions and electrostatic interactions (in the case of ionic and zwitterionic surfactants) between the surfactant polar heads. Micellization occurs when the attractive and the repulsive forces balance each other

*To whom correspondence should be addressed

(Israelachvili, 1991; Tanford, 1980).

Micelles are labile entities formed by the noncovalent aggregation of individual surfactant monomers and can be spherical, cylindrical, or planar (discs or bilayers). Micelle shape and size can be controlled by changing the surfactant chemical structure as well as by varying solution conditions, including temperature, overall surfactant concentration, surfactant composition (in the case of mixed surfactant systems), ionic strength, and pH. In particular, depending on the surfactant type and on the solution conditions, spherical micelles can grow one-dimensionally into cylindrical micelles or two-dimensionally into bilayers or discoidal micelles. Micelle growth is controlled primarily by the surfactant heads, since both one-dimensional and two-dimensional growth require bringing the surfactant heads closer to each other in order to reduce the available area per surfactant molecule at the micelle surface, and hence the curvature of the micelle surface (see Figure 2) (Chevalier and Zemb, 1990; Puvvada and Blankschtein, 1990).

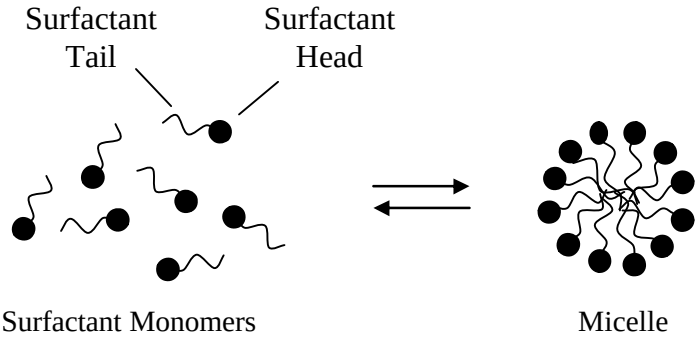

Figure 1: Schematic illustration of the reversible monomer-micelle thermodynamic equilibrium (Based on Liu et al., 1996). The black circles represent the surfactant heads (hydrophilic moieties) and the black curved lines represent the surfactant tails (hydrophobic moieties). When micelles form in aqueous solution above the CMC, the surfactant monomers aggregate (self-assemble) with the tails inside the micelle shielded from water and the heads at the micelle surface in contact with water.

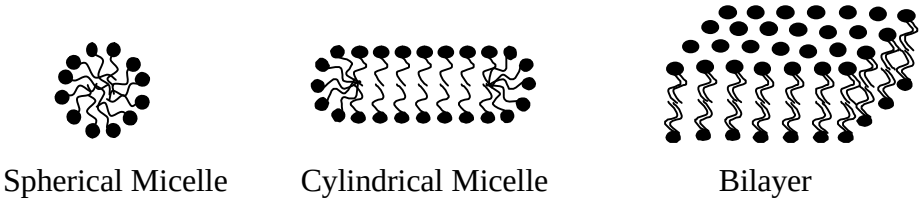

Figure 2: Schematic illustration of the three most commonly observed geometrical shapes of surfactant micelles in aqueous solution.

At certain surfactant concentrations and temperatures, some micellar solutions can macroscopically phase separate into a micelle-rich phase and a micelle-poor phase. The phase separation behavior results from the competition between internal energy effects, which promote the separation of micelles from water, and entropic effects, which promote the miscibility of micelles in water (Liu et al., 1996). Since the two coexisting micellar phases are at surfactant concentrations that exceed the CMC, micelles are present in both phases. For example, upon increasing the temperature, an aqueous solution of the nonionic surfactant n-decyl tetra(ethylene oxide) ($C_{10}E_4$) undergoes macroscopic phase separation into a top, micelle-rich phase and a bottom, micelle-poor phase, as shown schematically in Figure 3 (Liu et al., 1996). In this system, both phases contain cylindrical $C_{10}E_4$ micelles, which can be modeled as micelles having a cylindrical body capped by two hemispherical micelles at the ends (Puvvada and Blankschtein, 1990; Zoeller et al., 1997). However, the $C_{10}E_4$ micelles in the top phase are larger and more abundant than those in the bottom phase. Based on this difference in the physicochemical environment of the two coexisting micellar phases, and since both micellar phases contain about or above 90 wt% of water, the two-phase aqueous nonionic $C_{10}E_4$ micellar system provides a potential alternative for protein purification using principles of liquid-liquid extraction (Liu et al., 1996).

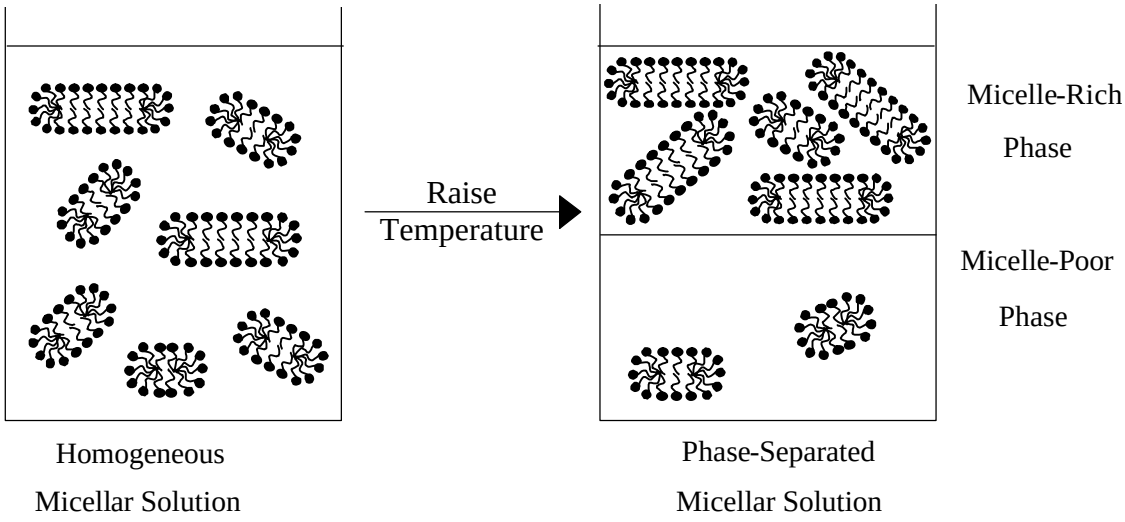

Figure 3: Schematic illustration of phase separation in the aqueous $C_{10}E_4$ micellar system upon increasing the temperature (Based on Liu et al., 1998). The $C_{10}E_4$ micellar solution has a single phase at low temperatures and phase separates with an increase in temperature into a top, micelle-rich phase and a bottom, micelle-poor phase.

Knowledge of the coexistence curve is essential when working with two-phase aqueous micellar systems. The coexistence curve represents the boundary separating the one-phase region from the two-phase region of an appropriate phase diagram (see below). As one traverses this boundary from the one-phase region to the two-phase region, the solution becomes turbid, signaling the onset of phase separation (Rangel-Yagui et al., 2003). For examples of experimentally determined coexistence curves corresponding to the aqueous $C_{10}E_4$ micellar system and to the aqueous mixed ($C_{10}E_4$/C_{10}TAB) micellar system, see Figures 5 and 7, respectively.

When compared to the extensively studied two-phase aqueous polymer systems (Abbott et al., 1990, 1991, 1992; Albertsson, 1986), two-phase aqueous micellar systems offer a number of unique and desirable features. These include: (i) the self-assembling nature of micelles which enables one to control and optimize the partitioning behavior by tuning various micelle characteristics, and (ii) the ability of micelles to offer simultaneously both hydrophobic and hydrophilic environments to biomolecules, allowing selectivity in partitioning based on the hydrophobicity of the biomolecules (Liu et al., 1996).

Bordier was the first to investigate the use of two-phase aqueous micellar systems for the purification of biomolecules. Using the two-phase aqueous Triton X-114 (a nonionic surfactant) micellar system, Bordier showed that hydrophilic proteins (serum albumin, catalase, ovalbumin, concavalin A, myoglobin, and cytochrome *c*) partition preferentially into the micelle-poor phase, while hydrophobic or integral membrane proteins (acetylcholinesterase, bacteriorhodopsin, and cytochrome *c* oxidase) partition preferentially into the micelle-rich phase (Bordier, 1981). Based on Bordier's work, the purification/extraction of other hydrophobic biomolecules such as piruvate oxidase, chlorophyll, and cholesterol oxidase, were studied (Minuth et al., 1996; Sanchez-Ferrer et al., 1994; Zhang and Hager, 1987).

The potential of separating hydrophilic biomolecules in two-phase aqueous micellar systems based on size differences was first recognized by Blankschtein and co-workers, who studied the partitioning of several water soluble proteins (ovalbumin, bovine serum albumin, cytochrome *c*, catalase, and soybean trypsin inhibitor) in the two-phase aqueous $C_{10}E_4$ micellar system (Nikas et al., 1992; Liu et al., 1996). In addition, a theoretical description was developed to model the partitioning behavior of hydrophilic proteins in two-phase aqueous $C_{10}E_4$ micellar systems (Nikas et al., 1992). More recently, this theoretical description was extended to model the partitioning of hydrophilic proteins in two-phase aqueous mixed (nonionic/ionic)

micellar systems, where electrostatic interactions between the charged mixed micelles and the charged proteins were accounted for (Kamei et al., 2002a). At the practical level, it was shown that electrostatic interactions between charged proteins and oppositely charged mixed micelles can be exploited to enhance the yield and selectivity of two-phase aqueous mixed (nonionic/ionic) micellar systems for the purification of proteins and viruses (Kamei et al., 2002b; Rangel-Yagui et al., 2003).

Although it is well known that ionic surfactants can bind to proteins and induce denaturation, this effect has been shown to depend on the type and concentration of the ionic surfactant (Cardamone et al., 1994; Gelamo and Tabak, 2000). Therefore, when working with a two-phase aqueous mixed (nonionic/ionic) micellar system, the amount of ionic surfactant added should be sufficiently high to induce a significant change in the protein partitioning behavior, but sufficiently low to prevent severe denaturation of the protein (Kamei et al., 2002a,b).

Similar to the $C_{10}E_4$/buffer micellar system, the mixed $C_{10}E_4$/C_{10}TAB/buffer micellar system studied exhibits a single, homogeneous micellar phase at low temperatures that can macroscopically separate into a top, micelle-rich phase, and a bottom, micelle-poor phase as the temperature is increased (Rangel-Yagui et al., 2003). However, unlike the micelles present in the $C_{10}E_4$/buffer micellar system, every micelle in the two-phase aqueous $C_{10}E_4$/C_{10}TAB/buffer micellar system is a *mixed micelle* composed of both $C_{10}E_4$ and C_{10}TAB, as shown schematically in Figure 4.

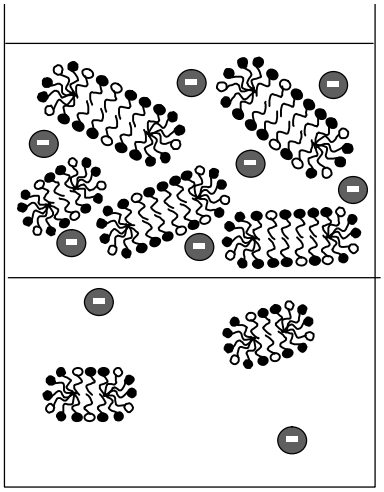

Figure 4: Schematic illustration of a net negatively charged hydrophilic protein (G6PD in the present case) partitioning in the two-phase aqueous mixed ($C_{10}E_4$/C_{10}TAB) micellar system (Based on Liu et al., 1998). The black and white circles represent the hydrophilic heads of the $C_{10}E_4$ and the C_{10}TAB surfactant molecules, respectively. Note that every micelle in the mixed $C_{10}E_4$/C_{10}TAB micellar system is a mixed micelle composed of both surfactant types. The gray circles represent the net negatively charged hydrophilic proteins (G6PD), which may partition preferentially into the top micelle-rich phase due to the attractive electrostatic interactions with the positively charged ($C_{10}E_4$/C_{10}TAB) mixed micelles.

The enzyme studied in this paper, glucose-6-phosphate dehydrogenase (G6PD) (EC.1.1.1.49), is the first enzyme of the pentose phosphate pathway and is very interesting as an analytical reagent, being used in various quantitative assays, including the measurement of creatin-kinase activity, hexoses concentrations, and as a marker for enzyme immunoassays (Bassi et al., 1999; Lojudice et al., 2001). The industrial purification of the hydrophilic enzyme G6PD involves expensive techniques, such as affinity chromatography and ion-exchange chromatography (Champluvier and Kula, 1992; Chang and Chase, 1996; McCreath et al., 1995), making the search for a simpler and more economical method to purify G6PD important and desirable.

The objective of this paper is to review the work by Blankschtein and co-workers on the use of two-phase aqueous micellar systems for the purification of hydrophilic proteins and at the same time discuss

very recent work on the partitioning of G6PD using i) two-phase aqueous micellar system composed of the nonionic surfactant n-decyl tetra(ethylene oxide) ($C_{10}E_4$), and (ii) two-phase aqueous mixed micellar system composed of $C_{10}E_4$ and the cationic surfactant decyltrimethylammonium bromide (C_{10}TAB). The remainder of the paper is organized as follows. In the sequence, we present a brief review of the excluded-volume and the electrostatic theories of protein partitioning in two-phase aqueous micellar systems. Following, we review as well as present new results of our experimental and theoretical studies of the partitioning behavior of the enzyme G6PD in (i) the two-phase aqueous $C_{10}E_4$ micellar system and (ii) the two-phase aqueous mixed ($C_{10}E_4$/C_{10}TAB) micellar system. Finally, we present our conclusions and provide additional perspectives.

REVIEW OF THE EXCLUDED-VOLUME AND THE ELECTROSTATIC THEORIES OF PROTEIN PARTITIONING IN TWO-PHASE AQUEOUS MICELLAR SYSTEMS

The partitioning behavior of a protein in a two-phase aqueous micellar system can be quantified in terms of the protein partition coefficient, K_p, defined as follows:

$$K_p \equiv \frac{C_{p,t}}{C_{p,b}} \tag{1}$$

where $C_{p,t}$ and $C_{p,b}$ are the protein concentrations in the top, micelle-rich phase and in the bottom, micelle-poor phase, respectively.

For a hydrophilic protein, the partitioning behavior in two-phase aqueous nonionic micellar systems composed of cylindrical micelles was modeled by Blankschtein and co-workers using excluded-volume considerations (Nikas et al., 1992). According to this theory, the partitioning of proteins is governed primarily by repulsive, steric, excluded-volume (EV) interactions between the globular hydrophilic proteins and the non-charged micelles. In that case, the proteins partition preferentially into the micelle-poor phase, where they experience fewer excluded-volume interactions with the micelles. In addition, the protein partitioning behavior can also be understood from a purely entropic point-of-view, since the hydrophilic proteins can sample a larger number of configurations in the micelle-poor phase due to the larger available free volume (Lue and Blankschtein, 1996). Based on this excluded-volume hypothesis, statistical thermodynamics was used to derive an expression for the protein partition coefficient in two-phase aqueous nonionic micellar systems. It was found that, under conditions of low protein concentration, noncharged surfactants, and low salt concentration, the partition coefficient is given by (Lue and Blankschtein, 1996; Nikas et al., 1992):

$$K_p^{EV} = \exp\left[-(\phi_t - \phi_b)\left(1 + \frac{R_p}{R_o}\right)^2\right] \tag{2}$$

where ϕ_t and ϕ_b are the surfactant volume fractions in the top and bottom phases, respectively, R_p is the hydrodynamic radius of the protein, and R_o is the cross-sectional radius of each cylindrical micelle.

In the case of G6PD, R_p in Eq. (2) was estimated to be 68 Å according to the dimensions of the enzyme isomorphous crystal (Rowland et al., 1994). In general, the cross-sectional radius of a cylindrical micelle, R_o in Eq. (2), can be estimated from the optimal length of the surfactant molecule (Puvvada and Blankschtein, 1990; Tanford, 1980). In particular, the R_o value corresponding to a cylindrical $C_{10}E_4$ micelle was estimated to be 21 Å based on the molecular model of micellization developed by Puvvada and Blankschtein (1990). The ($\phi_t - \phi_b$) value in Eq. (2) can be obtained from the experimentally determined coexistence curve, as discussed below.

The partitioning behavior of hydrophilic proteins in two-phase aqueous mixed (nonionic/ionic) micellar systems cannot be quantified using Eq. (2), because electrostatic interactions operating between the charged mixed micelles and the charged proteins were not accounted for in the derivation of Eq. (2). Therefore, a detailed protein partitioning theory that incorporates both excluded-volume and electrostatic interactions was developed recently (Kamei et al., 2002a), based on electrostatic considerations in the context of a molecular-thermodynamic theory of mixed surfactant micellization developed earlier (Shiloach and Blankschtein, 1998; Zoeller and Blankschtein, 1995; Zoeller et al., 1996). According to the new partitioning theory, the partition coefficient of a hydrophilic protein in two-phase aqueous mixed (nonionic/ionic) micellar systems can be expressed as follows (Kamei et al., 2002a):

$$K_p = K_p^{EV} K_p^{elec} \tag{3}$$

where K_p^{EV} denots the excluded-volume contribution to the protein partition coefficient and is given by Eq. (2), and K_p^{elec} denotes the electrostatic contribution to the protein partition coefficient and is given by (Kamei et al., 2002a):

$$K_p^{elec} = \exp\left[\frac{-\epsilon_w R_p}{2 R_o^2 k_B T}\left[\begin{array}{l}\left(\psi_{mic,t}^2 + \psi_p^2\right) I_t \phi_t - \\ \left(\psi_{mic,b}^2 + \psi_p^2\right) I_b \phi_b\end{array}\right]\right] \quad (4)$$

where ϵ_w is the dielectric constant of water, k_B is the Boltzmann constant, T is the absolute temperature, $\psi_{mic,x}$ is the electrostatic potential at the surface of each micelle in phase x (top (t) or bottom (b)), ψ_p is the electrostatic potential at the surface of the protein, and I_x is an integral over the entire volume of phase x, reflecting electrostatic interactions between a charged mixed micelle and a charged protein in phase x, given by the following expression (Kamei et al., 2002a):

$$I_x = \int_{R_{min}}^{\infty}\left[\begin{array}{l}\dfrac{2\psi_{mic,x}\psi_p}{\psi_{mic,x}^2 + \psi_p^2}\ln\left[\dfrac{1+\exp\left(-\kappa\left(r-R_o-R_p\right)\right)}{1-\exp\left(-\kappa\left(r-R_o-R_p\right)\right)}\right] + \\ +\ln\left[1-\exp\left(-2\kappa\left(r-R_o-R_p\right)\right)\right]\end{array}\right] r\,dr \quad (5)$$

where κ is the inverse of the Debye-Hückel screening length based on the buffer salt ions in the aqueous hypersolvent, and r is the radial distance from the axis of symmetry of the cylindrical micelle. The lower limit of integration in Eq. (5), R_{min}, corresponds to the minimum radial distance between the cylindrical axis of the micelle and the center of the protein and is given by $R_{min} = R_o + R_p + d_{min}$, where d_{min} = 6 Å and corresponds to the distance of closest approach between the micelle and the protein (Rangel-Yagui et al., 2003).

The expressions for $\psi_{mic,x}$ (x = t or b) and ψ_p (both in the cgs system of units) are given by (Bockris and Reddy, 1970; Hiemenz and Rajagopalan, 1997):

$$\psi_{mic,x} = \frac{4\pi\sigma_x}{\kappa\epsilon_w} \quad (6)$$

and

$$\psi_p = \frac{4\pi\sigma_p R_p}{\epsilon_w(1+\kappa R_p)} \quad (7)$$

where σ_x is the surface charge density of each micelle in phase *x* and σ_p is the surface charge density of the protein (G6PD in the present case). The surface charge density of G6PD was calculated by modeling the enzyme as a sphere, having a net charge of –42.2 at pH 7.2, as estimated using the Henderson-Hasselbalch equation (Stryer, 1988). The surface charge density of each micelle in phase *x* was calculated according to the following equation (Rangel-Yagui et al., 2003):

$$\sigma_x = \frac{\alpha_{mic} z_{cationic} e \ell_{c,x}^2}{2\ell_{cationic,x}\left[(1-\alpha_{mic})V_{tail,C_{10}E_4} + \alpha_{mic} V_{tail,C_{10}TAB}\right]} \quad (8)$$

where α_{mic} is the micelle composition of the cationic surfactant in terms of moles (α_{mic} = $[C_nTAB]_{mic}$ / ($[C_nTAB]_{mic}$+$[C_{10}E_4]_{mic}$)) in phase x (t or b), $z_{cationic}$ = +1 is the valence of a cationic surfactant molecule, e is the electronic charge, $\ell_{c,x}$ is the core radius of the mixed micelle in phase x, $\ell_{cationic,x}$ is the length of a cationic surfactant molecule in each micelle in phase x, and $V_{tail,C_{10}E_4}$ = $V_{tail,C_{10}TAB}$ = 269.5 Å (Tanford, 1980) are the volumes of the hydrophobic (C_{10}) tails of the nonionic and the cationic surfactants, respectively.

MATERIALS AND METHODS

Materials

The nonionic surfactant n-decyl tetra(ethylene oxide) ($C_{10}E_4$, lot no. 6011) was purchased from Nikko Chemicals (Tokyo, Japan). The cationic surfactant *n*-decyltrimethylammonium bromide (C_{10}TAB, lot no. OGI01) was purchased from TCI-America (Portland, OR). The glucose-6-phosphate dehydrogenase (G6PD) from *Leuconostoc mesenteroides* (lot no. 50K8612), glucose-6-phosphate (lot no. 40K7014), and β-nicotinamide adenine dinucleotide phosphate (β-$NADP^+$, lot no. 80K7046) were purchased from Sigma (St. Louis, MO). The other reagents were all of analytical grade. All these materials were used as received. In all the experiments, we utilized McIlvaine's buffer, at pH 7.2, consisting of 16.4 mM disodium phosphate and 1.82 mM citric acid in water purified through a Millipore Milli-Q ion-exchange system (Bedford,

MA). The glassware used was washed in a 50:50 ethanol:1 M sodium hydroxide bath, followed by a 1 M nitric acid bath, rinsed copiously with Milli-Q water, and finally dried in an oven.

Determination of G6PD Concentrations by Enzymatic Assay

The determination of G6PD concentrations in aqueous surfactant solutions was based on a well-established enzymatic assay (Bergmeyer, 1983). To prevent phase separation during the assay, which occurs at ~ 18 ^{o}C (Nikas et al., 1992), the enzymatic assay was carried out at a temperature of 15 ^{o}C. The activity of G6PD was measured by determining the rate of NADPH formation, which absorbs ultraviolet light at 340 nm, using a Shimadzu UV-160U spectrophotometer. One G6PD unit was defined as the amount of enzyme that catalyzes the reduction of 1 μmol of $NADP^{+}$ per minute under the assay conditions.

Determination of Cationic Surfactant Concentrations by Titration

The concentration of cationic surfactant present in each coexisting micellar phase of the $C_{10}E_4$/C_{10}TAB/buffer micellar system was determined as described by Rangel-Yagui et al. (2003). Briefly, the sample was added to a 200 mL Erlenmeyer flask containing 5 mL of buffer solution, 2 drops of the tetrabromophenolphthalein ethyl ester indicator, and 1 mL of 1,2-dichloroethane. The mixture was titrated with a 10 mM sodium tetraphenylborate solution, and the cationic surfactant concentration was determined from the amount of sodium tetraphenylborate added, with a color change from sky blue to faint yellow in the organic phase (1,2-dichloroethane) signaling the endpoint of the titration.

G6PD Partitioning in Two-Phase Aqueous Micellar Systems

Buffered solutions, each with a total mass of 3 g, were prepared in graduated 10 mL test tubes by the addition of the desired amounts of $C_{10}E_4$, C_{10}TAB, and G6PD. Since the enzymatic assay for determination of G6PD concentrations is very sensitive, there was no need to use large amounts of the enzyme, and therefore, the overall G6PD concentration in each partitioning experiment was 0.0068 wt%. The solutions were well mixed and equilibrated at 4 ^{o}C in order for each solution to have a clear and homogeneous single phase. Subsequently, the solutions were placed in a thermo-regulated device, previously set at the desired temperature and maintained there for 3 hours to attain partitioning equilibrium. After partitioning equilibrium was attained, the two coexisting micellar phases that formed were withdrawn separately with great care, using syringe and needle sets and the G6PD concentrations in each phase were determined as described above. Each G6PD partitioning experiment was carried out in triplicate to verify reproducibility.

Mapping the Coexistence Curves

To better understand the G6PD partitioning behavior in the two-phase aqueous micellar systems and to be able to implement the recently developed theoretical descriptions of protein partitioning reviewed in this paper (Nikas et al., 1992; Kamei et al., 2002a), the surfactant concentrations in the two coexisting micellar phases must be known. Therefore, the coexistence curves of the systems studied were mapped out. For the $C_{10}E_4$/buffer micellar system, the coexistence curve was determined using the cloud-point method (Blankschtein et al., 1986). Specifically, this method consists of visually identifying the temperature, T_{cloud}, at which solutions of known $C_{10}E_4$ concentrations become turbid as the temperature is raised. The experimental coexistence curve is then obtained by plotting the observed values of T_{cloud} as a function of the corresponding surfactant concentrations, as shown in Figure 5.

For the $C_{10}E_4$/C_{10}TAB/buffer mixed micellar system at a given temperature and fixed pressure, the coexistence curve can be represented as a $C_{10}E_4$ concentration vs. C_{10}TAB concentration phase diagram, as shown in Figure 7. Accordingly, coexistence curves were mapped out at the same temperatures as those utilized in the G6PD partitioning experiments. To map each coexistence curve, the transition from a clear to a turbid solution was determined (by visual observation) as a function of the $C_{10}E_4$ and the C_{10}TAB concentrations. The coexistence curve was then obtained by plotting the $C_{10}E_4$ concentrations as a function of the corresponding C_{10}TAB concentrations at which phase separation was observed (under this condition, the solution goes from being clear to being turbid) (Rangel-Yagui et al., 2003).

For each point of the coexistence curves mapped out the sample was first stirred thoroughly, using a magnetic stirrer, to ensure temperature and

concentration homogeneity and subsequently observed for any signs of cloudiness with the stirrer turned off. A piece of paper written the word "clear" was placed behind the test tube to help visualizing the turbidity of the system. Specifically, the system was considered definitely turbid when it was not possible to read it.

RESULTS AND DISCUSSION

Coexistence Curve of the $C_{10}E_4$/Buffer Micellar System

The coexistence curve of the $C_{10}E_4$/buffer micellar system in the temperature – $C_{10}E_4$ concentration phase diagram was measured experimentally and is shown in Figure 5. The measured coexistence curve compares well with the one measured recently by Kamei et al. (2002a). The minimum of the coexistence curve is referred to as the lowest critical point, characterized by a critical temperature, T_c, and a critical surfactant concentration, X_c, where $T_c \tilde{}$ 19.0 ^oC and $X_c \tilde{}$ 2 wt % (see Figure 5). At any given temperature above T_c, a tie line is obtained by drawing a line parallel to the $C_{10}E_4$ concentration axis. For example, at 19.5 ^oC, the tie line corresponds to the dashed horizontal line in Figure 5, where at any $C_{10}E_4$ concentration along this tie-line, the $C_{10}E_4$ micellar solution will phase separate into a top phase and a bottom phase having $C_{10}E_4$ concentrations $C_{C_{10}E_4,t}$ = 5.3 wt % and $C_{C_{10}E_4,b}$ = 0.6 wt %, respectively, which correspond to the intersections of the tie line at 19.5 ^oC with the coexistence curve (see Figure 5). Since the top and bottom micellar phases have densities of approximately 1 g/mL, the $C_{10}E_4$ weight fractions can be approximated as volume fractions, and therefore, the $(\phi_t - \phi_b)$ value corresponds to the tie-line length divided by 100, to convert percents into fractions, i.e., $(\phi_t - \phi_b) = (C_{C_{10}E_4,t} - C_{C_{10}E_4,b})/100$.

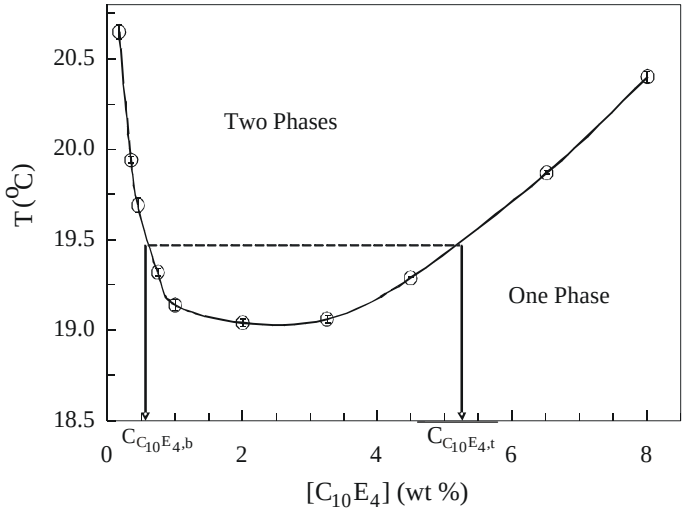

Figure 5: Experimentally determined coexistence curve of the $C_{10}E_4$/buffer micellar system. The region within the curve is the two-phase region, representing conditions under which the micellar solution separates into two macroscopic phases. The region outside the curve is the one-phase region, representing conditions under which the micellar solution is a single, homogeneous phase. The dashed line represents a tie line corresponding to 19.5 ^oC. At T = 19.5 ^oC, a $C_{10}E_4$ micellar solution having any $C_{10}E_4$ concentration along the tie line will phase separate into top and bottom phases having concentrations $C_{C_{10}E_4,t}$ = 5.8 wt % and $C_{C_{10}E_4,b}$ = 0.6 wt %, respectively. The error bars represent 95% confidence levels for the measurements.

According to Eq. (2) discussed in the theoretical review, for a given hydrophilic protein (fixed R_P) and a given surfactant type (fixed R_o), the larger the value of $(\phi_t - \phi_b)$, the lower the value of K_p, and therefore, the better the protein partitioning behavior. One should keep in mind that the best protein partitioning is attained when K_p approaches zero, i.e., when the target protein partitions very extremely to one of the phases (say, to the bottom phase). The coexistence curve in Figure 5 shows that the value of $(\phi_t - \phi_b)$ increases as the temperature increases relative to T_c. As a result, for $T > T_c$, K_p should

decrease with an increase in temperature (see Eq.(2)).

Partitioning of G6PD in the $C_{10}E_4$/Buffer Micellar System

The partitioning behavior of the enzyme G6PD in the $C_{10}E_4$/buffer micellar system was studied experimentally at various temperatures. The measured G6PD partition coefficients (K_{G6PD}) and the corresponding G6PD activity balances (AB_{G6PD}) are presented in Table 1, where the activity balance is defined as

$$AB_{G6PD} = \frac{C_{G6PD,t}V_t + C_{G6PD,b}V_b}{C_{G6PD,i}V_i} \times 100\% \qquad (9)$$

In Eq. (9), $C_{G6PD,t}$, $C_{G6PD,b}$, and $C_{G6PD,i}$ are the G6PD concentrations in the top phase, the bottom phase, and the G6PD solution prior to phase separation, respectively, and V_t, V_b, and V_i are the volumes of the top phase, the bottom phase, and the G6PD solution prior to phase separation, respectively.

Table 1 shows that the G6PD activity balance closed to approximately 100% in all the partitioning experiments, demonstrating that G6PD is stable in the $C_{10}E_4$/buffer micellar system. The measured G6PD partition coefficients are less than one in all the cases studied and become smaller at the higher temperatures, as expected based on the excluded-volume theory presented.

The (ϕ_t - ϕ_b) values reported in Table 1 were utilized to predict the G6PD partition coefficients using Eq. (2). Figure 6 presents a comparison between the experimental K_{G6PD} values (circles) and the predicted K_{G6PD} values (line) as a function of (ϕ_t - ϕ_b), and as can be seen, reasonable quantitative agreement is obtained. The observed deviation between experiment and theory may be due to modeling G6PD as an effective hard sphere, instead of as an ellipsoid (Rowland et al., 1994), which may have led to an overestimation of the G6PD-micelle excluded-volume interactions, and hence to lower predicted values of K_{G6PD}.

Table 1: Experimental G6PD partitioning results at various temperatures in the two-phase aqueous $C_{10}E_4$/buffer micellar system: f_t and f_b correspond to the surfactant volume fractions in the top and the bottom micellar phases, respectively; K_{G6PD} is the G6PD partition coefficient; and AB_{G6PD} is the G6PD activity balance. The errors represent 95% confidence levels for the measurements.

Experiment	T (^oC)	[$C_{10}E_4$] (wt %)	($\phi_t - \phi_b$)	K_{G6PD}	AB_{G6PD} (%)
1	19.5	2.50	0.046	0.53 ± 0.04	97 ± 9
2	20.0	3.60	0.066	0.36 ± 0.00	104 ± 4
3	20.3	4.00	0.072	0.34 ± 0.02	107 ± 7
4	20.4	3.25	0.079	0.33 ± 0.01	108 ± 7
5	21.5	3.00	0.105	0.20 ± 0.04	101 ± 6
6	22.0	5.00	0.118	0.10 ± 0.01	101 ± 2

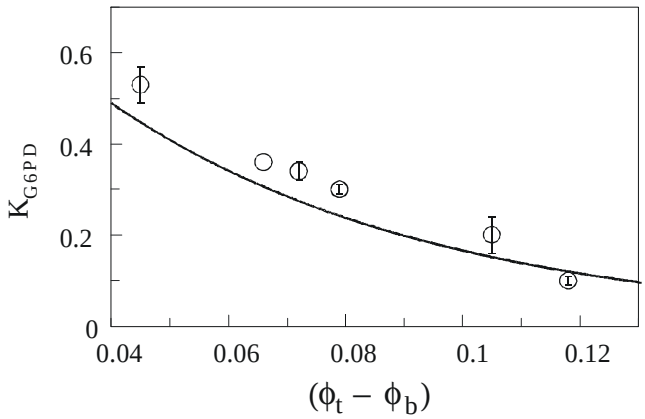

Figure 6: Comparison between the theoretically predicted (solid line) and the experimentally measured (open circles) G6PD partition coefficients (K_{G6PD}) in the $C_{10}E_4$/buffer micellar system as a function of ($\phi_t - \phi_b$), where ϕ_t and ϕ_b are the $C_{10}E_4$ volume fractions in the top and bottom phases, respectively. The error bars represent 95% confidence levels for the measurements.

As shown in Table 1 and Figure 6, the partitioning of the hydrophilic enzyme G6PD in the two-phase aqueous $C_{10}E_4$ micellar system results in K_{G6PD} values which are less than one, owing to the preferential partitioning of G6PD to the bottom, micelle-poor phase (see Eq. (2)). On the other hand, hydrophobic proteins are expected to partition preferentially to the top, micelle-rich phase, since the micelle core offers a hydrophobic environment to these proteins and the micelles are more abundant in the top phase. Therefore, the two-phase aqueous $C_{10}E_4$ micellar system can be considered as an interesting alternative for separating the enzyme G6PD from hydrophobic proteins and other hydrophobic cell components.

In addition, in many practical recovery/purification processes, there is a need to separate a target hydrophilic biomolecule (for example, G6PD) from other water-soluble proteins. Accordingly, the possibility of creating a two-phase aqueous micellar system with other types of micelle-protein interactions, in addition to those of the excluded-volume type, which could drive the target protein (say, G6PD) preferentially to the top phase while the excluded-volume interactions drive the other hydrophilic proteins preferentially to the bottom phase, is worth exploring. With this need in mind, a new two-phase aqueous mixed (nonionic/cationic) micellar system was studied, and the results obtained when the enzyme G6PD is partitioned in this system are discussed next.

Coexistence Curve of the $C_{10}E_4/C_{10}TAB$/Buffer Mixed Micellar System

The coexistence curves corresponding to the $C_{10}E_4/C_{10}TAB$/buffer mixed micellar system were mapped out at the same temperatures as those utilized in the G6PD partitioning experiments in this system (26.7 °C and 30.0 °C). By connecting the two points on the experimentally mapped coexistence curve corresponding to the cationic surfactant concentrations in each coexisting phase of the $C_{10}E_4/C_{10}TAB$ micellar system (measured using the titration method described in the Materials and Methods Section), the concentration of the $C_{10}E_4$ nonionic surfactant in each phase could be determined as well as the respective tie line, which should pass through the point corresponding to the experimental G6PD partitioning condition (namely, to the total $C_{10}E_4$ and $C_{10}TAB$ concentrations at the operating temperature).

Figure 7 shows the experimentally measured coexistence curves and tie lines for the $C_{10}E_4/C_{10}TAB$/buffer mixed micellar system at 26.7°C (A) and at 30.0°C (B). In each coexistence curve, the filled circles denote the compositions of the top and bottom phases corresponding to the partitioning experiment carried out at the same temperature at which the coexistence curve was mapped out. The dashed lines connecting these points are the operating tie lines and the open circles correspond to the overall solution compositions of the partitioning experiments. As can be seen, there is good agreement between the compositions of the top and bottom phases and the solution composition for each partitioning experiment, since in each case, the tie line obtained passes through the point corresponding to the experimental phase separation condition, within the experimental uncertainty.

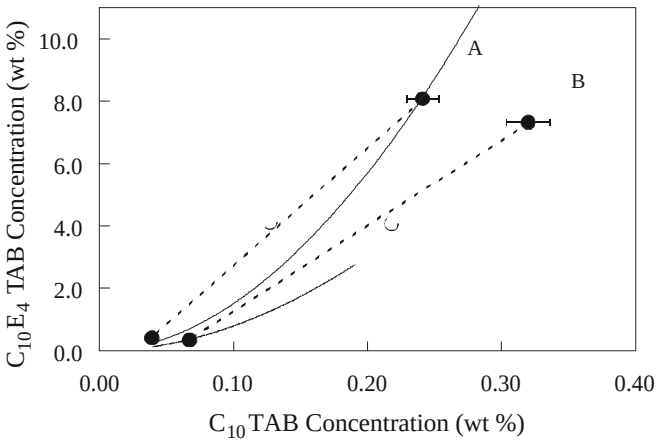

Figure 7: Experimentally determined coexistence curves of the $C_{10}E_4/C_{10}TAB$/buffer mixed micellar system at 26.7 °C (A) and 30.0 °C (B) with their respective tie lines, represented by the dashed lines. The intersections of the tie lines with the coexistence curves (filled circles) were obtained based on the $C_{10}TAB$ concentrations determined in the top and bottom phases. The open circles represent the actual solution compositions at which G6PD was partitioned at the respective temperatures. The error bars represent 95% confidence levels for the $C_{10}TAB$ concentration measurements.

Partitioning of G6PD in the $C_{10}E_4/C_{10}TAB$/Buffer Mixed Micellar System

The G6PD partitioning experiments in the $C_{10}E_4/C_{10}TAB$/buffer mixed micellar system were conducted with a total surfactant concentration of 128 mM at solution compositions α_{sol} = 0.035 and 0.06, where $\alpha_{sol} = [C_{10}TAB]/([C_{10}TAB]+[C_{10}E_4])$ is the actual solution molar fraction of the cationic surfactant. For α_{sol} = 0.035, the partitioning was carried out at 26.7 °C, and for α_{sol} = 0.06, it was carried out at 30.0 °C in order to observe phase separation. Figure 8A shows the measured K_{G6PD} values, and Figure 8B shows the measured AB_{G6PD} values obtained in the $C_{10}E_4/C_{10}TAB$/buffer mixed micellar system. Figure 8A shows that, at both solution compositions, the K_{G6PD} values are greater than one, reflecting the effect of the attractive electrostatic interactions between the positively charged $C_{10}E_4/C_{10}TAB$ mixed micelles and the net negatively charged enzyme G6PD on its partitioning behavior. The highest G6PD partition coefficient, K_{G6PD} = 7.7, was attained with α_{sol} = 0.06, while with α_{sol} = 0.035, a value of K_{G6PD} = 1.8 was attained. Clearly, Figure 8A shows that increasing the cationic surfactant concentration results in higher G6PD partition coefficient values due to the stronger attractive electrostatic interactions between the oppositely charged mixed micelles and G6PD.

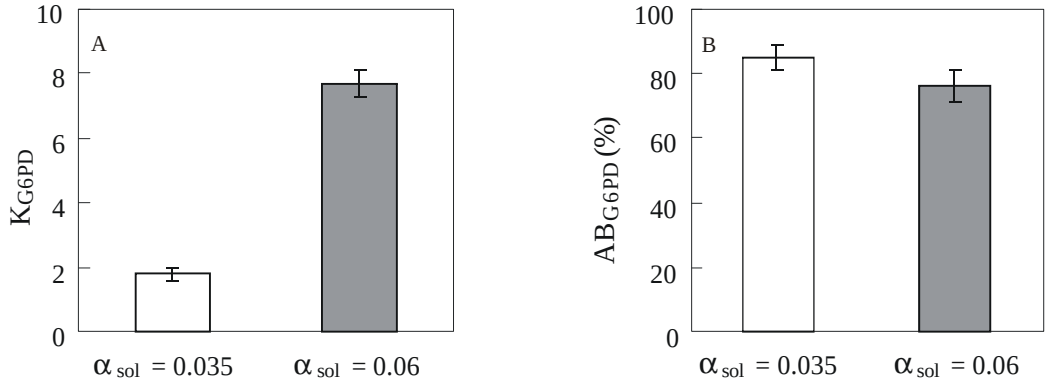

Figure 8: A – Experimentally measured G6PD partition coefficients (K_{G6PD}), and B – experimentally measured activity balances (AB_{G6PD}) in the $C_{10}E_4/C_{10}TAB$/buffer mixed micellar system at 26.7 °C (α_{sol} = 0.035, open bars) and 30.0 °C (α_{sol} = 0.06, gray bars). The solution composition represents the fraction of cationic surfactant in relation to the total surfactant molar concentration ($\alpha_{sol} = [C_{10}TAB]/([C_{10}TAB]+[C_{10}E_4])$). The error bars represent 95% confidence levels for the measurements.

To further elucidate the importance of the electrostatic interactions in the partitioning behavior of the enzyme G6PD, the K_{G6PD} values obtained in the $C_{10}E_4/C_{10}TAB$/buffer mixed micellar system were compared to the ones in the $C_{10}E_4$/buffer micellar system under conditions where the excluded-volume interactions operating between the micelles and the enzyme G6PD were the same for both systems. Note that the excluded-volume interactions can be maintained constant if the same $(\phi_t - \phi_b)$ value is maintained for the $C_{10}E_4/C_{10}TAB$/buffer mixed micellar system and for the $C_{10}E_4$/buffer micellar system. Based on the coexistence curves obtained for the $C_{10}E_4/C_{10}TAB$/buffer mixed micellar system, the $(\phi_t - \phi_b)$ values were estimated to be 0.072 at T = 30.0 °C and 0.079 at T = 26.7 °C. As can be seen in Table 1, similar $(\phi_t - \phi_b)$ values are observed in experiments 3 and 4, respectively, in the $C_{10}E_4$/buffer micellar system. As can also be seen in Table 1, the measured K_{G6PD} values corresponding to experiments 3 and 4 are significantly smaller than those in the $C_{10}E_4/C_{10}TAB$/buffer mixed micellar system under the same excluded-volume condition, demonstrating that the net negatively charged enzyme G6PD is indeed attracted electrostatically to the top, mixed micelle-rich phase of the $C_{10}E_4/C_{10}TAB$/buffer mixed micelar system, which contains a larger number of positively charged $C_{10}E_4/C_{10}TAB$ mixed micelles, thus resulting in higher partition coefficients.

The G6PD activity balances in Figure 8B, when compared to the results in Table 1, reveal that G6PD is more stable in the $C_{10}E_4$/buffer micellar than in the $C_{10}E_4/C_{10}TAB$/buffer mixed micellar system. In general, activity balance values lower than 100% indicate that denaturation of G6PD took place at

some level. This observed denaturation results from the presence of the cationic surfactant $C_{10}TAB$ and is proportional to its concentration. Accordingly, a higher AB_{G6PD} value was observed at lower concentrations of the cationic surfactant $C_{10}TAB$ (α_{sol} = 0.035) (see Figure 8B). Nevertheless, it is always possible to maintain a higher G6PD activity balance by adding less cationic surfactant at the expense of attaining lower K_{G6PD} values.

For a better understanding of the practical advantage of adding more cationic surfactant, the value of the G6PD yield in the top, mixed micelle-rich phase ($Y_{G6PD,t}$) was calculated for each condition examined, where $Y_{G6PD,t}$ is defined as follows:

$$Y_{G6PD,t} = \frac{C_{G6PD,t} V_t}{C_{G6PD,i} V_i} \times 100\% \quad (10)$$

In the $C_{10}E_4/C_{10}TAB$/buffer mixed micellar system at α_{sol} = 0.035, a $Y_{G6PD,t}$ value of 48% was obtained, while at α_{sol} = 0.06, a $Y_{G6PD,t}$ value of 71% was obtained. Therefore, an α_{sol} of 0.06 provides a better balance between the denaturing effect of $C_{10}TAB$ on G6PD and the electrostatic attractions between the positively charged $C_{10}E_4/C_{10}TAB$ mixed micelles and the net negatively charged enzyme G6PD. In other words, the higher stability of G6PD in the $C_{10}E_4/C_{10}TAB$/buffer mixed micellar system at α_{sol} = 0.035 does not compensate for the lower K_{G6PD} value of 1.8, resulting in a relatively low $Y_{G6PD,t}$ value.

Theoretical K_{G6PD} values for the $C_{10}E_4/C_{10}TAB$/buffer mixed micellar system were predicted using a number of input parameters, including the micelle composition α_{mic}, ϕ_t, and ϕ_b. The values of ϕ_t and ϕ_b were obtained from the experimental coexistence curves in Figure 7. A molecular-thermodynamic theory of mixed surfactant micellization (Shiloach and Blankschtein, 1998; Zoeller and Blankschtein, 1995; Zoeller et al., 1996) was utilized to predict α_{mic} in each phase of the two-phase aqueous $C_{10}E_4/C_{10}TAB$/buffer mixed micellar system under the conditions studied. In Figure 9, the experimental K_{G6PD} values measured in the $C_{10}E_4/C_{10}TAB$/buffer mixed micellar system (gray bars) are compared to those predicted using the partitioning theory previously presented (open bars). As can be seen, there is a good agreement between the predicted and the experimental K_{G6PD} values.

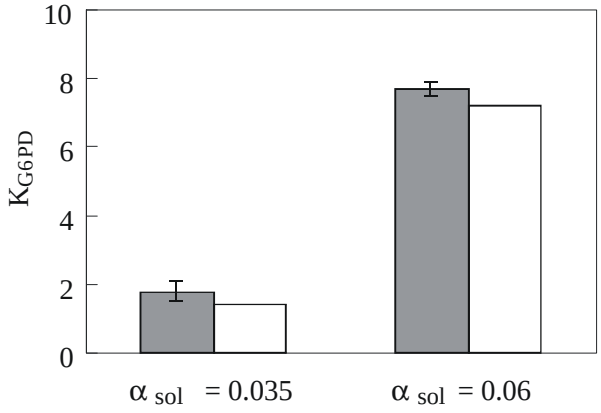

Figure 9: Comparison between the experimentally measured (gray bars) and the theoretically predicted (open bars) G6PD partition coefficients (K_{G6PD}) in the $C_{10}E_4/C_{10}TAB$/buffer mixed micellar system with an α_{sol} = 0.035 and an α_{sol} = 0.06. The error bars represent 95% confidence levels for the measurements.

CONCLUSIONS

Our recent experimental and theoretical work on the partitioning of the enzyme G6PD in two-phase aqueous micellar systems was reviewed and new results were presented. The partitioning of G6PD in the two-phase $C_{10}E_4$/buffer micellar system resulted in partition coefficient values less than one. This can be understood based on the theoretical assumption that the main driving force for the partitioning of hydrophilic proteins in the $C_{10}E_4$/buffer micellar system results from the excluded-volume interactions between the $C_{10}E_4$ micelles and the proteins. These interactions drive the proteins preferentially to the micelle-poor phase where they have a larger available free volume. Consequently, as expected, the hydrophilic enzyme G6PD was found to partition preferentially to the bottom, micelle-poor phase of the $C_{10}E_4$/buffer micellar system.

On the other hand, the partitioning of G6PD in the $C_{10}E_4/C_{10}TAB$/buffer mixed micellar system resulted in partition coefficient values greater than one, as well as significantly greater than those observed in the $C_{10}E_4$/buffer system. This finding clearly demonstrates that the net negatively charged enzyme G6PD is attracted electrostatically to the top, mixed micelle-rich phase, which contains a larger number of positively charged $C_{10}E_4/C_{10}TAB$ mixed micelles than the bottom phase. The $C_{10}E_4/C_{10}TAB$/buffer mixed micellar system at an α_{sol} = 0.06 yielded the highest G6PD partition coefficient (K_{G6PD} = 7.7), resulting in a G6PD yield in the top phase of 71%.

The good agreement between the theoretically predicted and the experimentally measured K_{G6PD} values in both the nonionic $C_{10}E_4$/buffer micellar system and in the (nonionic/cationic) $C_{10}E_4/C_{10}TAB$/buffer mixed micellar system confirms the practical utility of the theory reviewed in this paper in guiding the implementation of optimal protein separation strategies.

In conclusion, two-phase aqueous micellar systems can be considered a promising new alternative for the purification of G6PD, as well as of other hydrophilic proteins. The two-phase aqueous nonionic micellar system could be utilized to purify a hydrophilic target protein that partitions preferentially to the bottom, micelle-poor phase (driven by excluded-volume interactions) from hydrophobic proteins, which partition preferentially to the top, micelle-rich phase, driven by hydrophobic interactions. The two-phase aqueous mixed (nonionic/ionic) micellar system, on the other hand, may be used to separate a target hydrophilic protein that partitions preferentially to the top, micelle-rich phase (driven by attractive electrostatic interactions with the charged mixed micelles) from other oppositely charged hydrophilic proteins that partition preferentially to the bottom, micelle-poor phase (driven by both repulsive electrostatic interactions and excluded-volume interactions with the charged mixed micelles).

Other interactions, such as affinity interactions, could also be exploited in two-phase aqueous micellar systems in order to improve the partitioning selectivity of biomolecules. Studies of target protein partitioning in two-phase aqueous micellar systems in the presence of other proteins as well as in real fermentation broths are also of fundamental and practical interest to understand the effect of the additional components on the partitioning behavior of the target protein. Work aimed at examining these interesting possibilities is in progress.

ACKNOWLEDGEMENTS

Carlota Rangel-Yagui is grateful for the financial support from CAPES - Coordenação de Aperfeiçoamento de Pessoal de Nível Superior. This research was supported in part by the Fundação de Amparo à Pesquisa do Estado de São Paulo – FAPESP. We are also grateful to Prof. Daniel Kamei (UCLA) and Henry Lam (MIT) for very useful discussions on experimental and theoretical aspects of two-phase aqueous micellar systems.

REFERENCES

Abbott, N.L., Blankschtein, D., and Hatton T.A., On Protein Partitioning in Two-Phase Aqueous Polymer Systems, Bioseparation, 1:191-225 (1990).

Abbott, N.L., Blankschtein, D., and Hatton T.A., Protein Partitioning in Two-Phase Aqueous Polymer Systems. 1. Novel Physical Pictures and a Scaling-Thermodynamic Formulation, Macromolecules, 24: 4334-4348 (1991).

Abbott, N.L., Blankschtein, D., and Hatton, T.A., Protein Partitioning in Two-Phase Aqueous Polymer Systems. 2. On the Free Energy of Mixing Globular Colloids and Flexible Polymers, Macromolecules, 25: 3917-3931 (1992).

Albertsson, P.Å., Partition of Cell Particles and Macromolecules, 3rd ed., New York: Willey-Interscience (1986).

Bassi, A.S., Tang, D.Q., and Bergougnou, M.A., Mediated Amperometric Biosensor for Glucose-6-Phosphate Monitoring Based on Entrapped Glucose-6-Phosphate Dehydrogenase, Mg^{+2} Ions, Tetracyanoquinodimethane, and Nicotinamide Adenine Dinucleotide Phosphate in Carbon Paste, Anal. Biochem., 268(2):223-228 (1999).

Bergmeyer, H.U., Methods of Enzymatic Analysis, Wheinheim: Velag Chemie, 3rd ed., 2nd vol., p.190-197 (1983).

Blankschtein, D., Thurston, G.M., and Benedek, G.B., Phenomenological Theory of Equilibrium Thermodynamic Properties and Phase Separation of Micellar Solutions, J. Chem. Phys., 85:7268-7288 (1986).

Bockris, J.O.M. and Reddy, A.K.N., Modern Electrochemistry, vol.1, New York: Plenum Press (1970).

Bordier, C., Phase Separation of Integral Membrane Proteins in Triton X-114 Solution, J. Biol. Chem., 256:1604-1607 (1981).

Cardamone, M., Puri, N.K., Sawyer, W.H., Capon, R.J., and Brandon, M.R., A Spectroscopic and

Equilibrium Binding Analysis of Cationic Detergent-Protein Interactions Using Soluble and Insoluble Recombinant Porcine Growth Hormone, Biochim. Biophys. Acta, 1206:71-82 (1994).

Champluvier, B. and Kula, M.R., Dye-Ligand Membranes as Selective Adsorbents for Rapid Purification of Enzymes: A Case Study, Biotechnol. Bioeng., 40:33-40 (1992).

Chang, Y.K. and Chase, H.A., Ion Exchange Purification of G6PDH from Unclarified Yeast Cell Homogenates Using Expanded Bed Adsorption, Biotechnol. Bioeng., 49(2):204-216 (1996).

Chevalier, Y. and Zemb, T., The Structure of Micelles and Microemulsions, Rep. Prog. Phys., 53:279-371 (1990).

Gelamo, E.L. and Tabak, M., Spectroscopic Studies on The Interaction of Bovine (BSA) and Serum (HSA) Albumins with Ionic Surfactants, Spectrochim. Acta A, 56:2255-2271 (2000).

Hiemenz, P.C. and Rajagopalan, R., Principles of Colloid and Surface Chemistry, 3rd ed., New York: Marcel Dekker (1997).

Israelachvili, J.N., Intermolecular and surface forces, 2ed., London: Academic (1991).

Kamei, D.T., Wang, D.I.C., and Blankschtein, D., Fundamental Investigation of Protein Partitioning in Two-Phase Aqueous Mixed (Nonionic/Ionic) Micellar Systems, Langmuir, 18:3047-3057 (2002a).

Kamei, D.T., King, J.A., Wang, D.I.C., and Blankschtein, D., Separating Lysozyme from Bacteriophage P22 in Two-Phase Aqueous Micellar Systems, Biotechnol. Bioeng.,. 80(2): 233-236 (2002b).

Liu, C.L., Nikas, Y.J., and Blankschtein, D., Novel Bioseparations Using Two-Phase Aqueous Micellar Systems, Biotechnol. Bioeng., 52:185-192 (1996).

Liu, C.L., Kamei, D.T., King, J.A., Wang, D.I.C., and Blankschtein, D., Separation of Proteins and Viruses Using Two-Phase Aqueous Micellar Systems, J. Chromatogr. B, 711:127-138 (1998).

Lojudice, F.H., Silva, D.P., Zanchin, N.I.T., Oliveira, C.C., and Pessoa-Jr, A., Overexpression of Glucose-6-Phosphate Dehydrogenase in Genetically Modified *Saccharomyces cerevisiae,* Appl. Biochem. Biotech., 91-93:161-169 (2001).

Lue, L. and Blankschtein, D., A Liquid-State Theory Approach to Modeling Solute Partitioning in Phase-Separated Solutions, Ind. Eng. Chem. Res., 35:3032-3043 (1996).

McCreath, G.E., Chase, H.A., Owen, R.O., and Lowe, C.R., Expanded Bed Affinity-Chromatography of Dehydrogenases from Bakers-Yeast Using Dye-Ligand Perfluoropolymer Supports, Biotechnol. Bioeng., 48(4):341-354 (1995).

Minuth, T., Hommes, J., and Kula, M.R., A Closed Concept for Purification of the Membrane-Bound Cholesterol Oxidase from *Nocardia rhodochrous* by Surfactant-Based Cloud-Point Extraction, Organic-Solvent Extraction and Anion-Exchange Chromatography, Biotechnol. Appl. Biochem., 23:107 (1996).

Nikas, Y.J., Liu, C.L., Srivastava, T., Abbott, N.L., and Blankschtein, D., Protein Partitioning in Two-Phase Aqueous Nonionic Micellar Solutions, Macromolecules, 25:4794-4806 (1992).

Puvvada, S. and Blankschtein, D., Molecular-Thermodynamic Approach to Predict Micellization, Phase Behavior, and Phase Separation of Micellar Solutions. I. Application to Nonionic Surfactants, J. Chem. Phys., 92(6):3710-3724 (1990).

Rangel-Yagui, C.O., Lam, H., Kamei, D.T., Wang, D.I.C., Pessoa-Jr, A., and Blankschtein, D., Glucose-6-Phosphate Dehydrogenase Partitioning in Two-Phase Aqueous Mixed (Nonionic/Cationic) Micellar Systems, Biotechnol. Bioeng., 82:445-456 (2003).

Rowland, P., Basak, A.K., Gover, S., Levy, H.R., and Adams, M.J., The Three-Dimensional Structure of Glucose-6-Phosphate Dehydrogenase from *Leuconostoc mesenteroides* Refined at 2.0 Å Resolution, Structure, 2(11):1073-1087 (1994).

Sanchez-Ferrer, A., Bru, R., and Garcia-Carmona, F., Phase Separation of Biomolecules in PoLyoxyethylene Glycol Nonionic Detergents, Critical Rev. Biochem. Mol. Biol., 29(4):275-313 (1994).

Shiloach, A. and Blankschtein, D., Measurement and Prediction of Ionic/Nonionic Mixed Micelle Formation and Growth, Langmuir, 14:7166-7182 (1998).

Stryer, L., Biochemistry, 3rd ed., New York: WH Freeman (1988).

Tanford, C., The Hydrophobic Effect: Formation of Micelles and Biological Membranes, 2nd ed., New York: Wiley (1980).

Zhang, T.F. and Hager, L.P., A Single-Step Large-Scale Purification of Pyruvate Oxidase, Arch. Biochem. Biophys., 257(2):485-487 (1987).

Zoeller, N. and Blankschtein, D., Development of User-Friendly Computer Programs to Predict Solution Properties of Single and Mixed Surfactant Systems, Ind. Eng. Chem. Res., 34: 4150-4160 (1995).

Zoeller, N., Shiloach, A., and Blankschtein, D., Predicting Surfactant Solution Behavior, Chemtech, 26(3): 24-31 (1996).

Zoeller, N., Lue, L., and Blankschtein, D., Statistical-Thermodynamic Framework to Model Nonionic Micellar Solutions, Langmuir, 13 (20):5258-5275 (1997).